

FULL PAPER

Synthesis, structure and *in vitro* anticancer, DNA binding and cleavage activity of palladium (II) complexes based on isatin thiosemicarbazone derivatives

Amna Qasem Ali¹ | Siang Guan Teoh² | Naser Eltaher Eltayeb³  | Mohamed B. Khadeer Ahamed⁴ | A.M.S. Abdul Majid⁴ | Arabya A.A. Almutaleb¹¹Chemistry Department, Faculty of Science, Sebha University, Sebha, Libya²School of Chemical Sciences, Universiti Sains Malaysia, Minden-11800, Pulau Pinang, Malaysia³Department of Chemistry, College of Sciences and Arts, King Abdulaziz University, Rabigh, Saudi Arabia⁴EMAN Research and Testing Laboratory, School of Pharmaceutical Sciences, Universiti Sains Malaysia, Minden-11800, Pulau Pinang, Malaysia**Correspondence**

Naser Eltaher Eltayeb, Department of Chemistry, College of Sciences and Arts, PO Box 344, King Abdulaziz University, Rabigh 21911, Saudi Arabia.

Email: netaha@kau.edu.sa

Funding information

Malaysian Government and Universiti Sains Malaysia for the RU research grant, Grant/Award Number: 1001/PKIMIA/815067; Ministry of Higher Education and the University of Sabha (Libya), Grant/Award Number: scholarship for AQA

Six novel palladium(II) complexes of a thiosemicarbazone Schiff base with isatin moiety (PdL1 to PdL6) were synthesized by the reaction of palladium(II) with the following: (*Z*)-2-(2-oxoindolin-3-ylidene)-*N*-phenylhydrazinecarbothioamide (L1H), (*Z*)-2-(5-methyl-2-oxoindolin-3-ylidene)-*N*-phenylhydrazinecarbothioamide (L2H), (*Z*)-2-(5-fluoro-2-oxoindolin-3-ylidene)-*N*-phenylhydrazinecarbothioamide (L3H), (*Z*)-*N*-methyl-2-(5-nitro-2-oxoindolin-3-ylidene)hydrazinecarbothioamide (L4H), (*Z*)-*N*-methyl-2-(5-methyl-2-oxoindolin-3-ylidene)hydrazinecarbothioamide (L5H) and (*Z*)-*N*-ethyl-2-(5-methyl-2-oxoindolin-3-ylidene)hydrazinecarbothioamide (L6H). The structures of these complexes were characterized using elemental analysis and infrared, UV–visible, ¹H NMR and mass spectroscopies. The structure of PdL5 was further characterized using single-crystal X-ray diffraction. The interaction of these complexes with calf thymus DNA was characterized with a high intrinsic binding constant ($K_b = 5.78 \times 10^4$ to $1.79 \times 10^6 \text{ M}^{-1}$), which reflected the intercalative activity of these complexes towards calf thymus DNA. This result was also confirmed from viscosity data. Electrophoresis studies revealed that complexes PdL1 to PdL6 could cleave DNA via an oxidative pathway in the presence of an external agent. Data obtained from an *in vitro* anti-proliferative study clearly established the anticancer potency of these compounds against the human colorectal carcinoma cell line HCT 116.

KEYWORDS

activityisatin, anti-proliferative, complexes, moietyoxidative, pathwaypalladium(II), studyintercalative

1 | INTRODUCTION

Square planar diamminedichloroplatinum(II), *cis*-[PtCl₂(NH₃)₂] or cisplatin, is one of the most potent anti-tumour drugs available for the therapeutic management of solid tumours, such as germ cell tumours and ovarian, lung, head, neck and bladder cancers.^[1,2] Given the numerous shortcomings of platinum complexes, anti-tumour drug research has been developing new compounds outside the usual

coordination sphere, such as organometallic complexes and complexes with metallic elements other than platinum. Among the transition metal complexes, palladium(II) complexes are very interesting candidates for alternative metal-based drugs because the coordination geometry and complex-forming processes of palladium(II) are highly similar to those of platinum(II).^[3] Palladium complexes show approximately 10⁴ to 10⁵ times higher reactivity, whereas their structural and equilibrium behaviours are very similar

to those of platinum complexes. Similarity between the coordination chemistry of platinum(II) and palladium(II) compounds also supports the theory that palladium complexes can act successfully as anti-tumour drugs.^[4] Thus, some palladium complexes with aromatic N-containing Schiff bases have shown very promising anti-tumour characteristics.^[3,5–7] With similar structural features, a study in 2015 investigated the interaction between isatin β -thiosemicarbazone and calf thymus DNA (CT DNA) using UV–visible absorption and fluorescence spectroscopy, as well as viscosity measurements. From the absorption spectrum of isatin β -thiosemicarbazone, as the concentration of DNA increases, a large degree of hypochromism develops in the spectrum which reflects the strong stacking interaction between the aromatic chromophore and the base pairs.^[8] Recently Patange *et al.* reported the synthesis and antimicrobial activity of palladium(II) complexes of thiosemicarbazone and semicarbazone derived from 5-bromoisatin. Those authors concluded that sulfur-containing ligands as well as their complexes are more active than their oxygen-containing counterparts.^[9]

The current paper describes the synthesis, physicochemical characterization and DNA binding activity of monopalladium(II) complexes with tridentate ligands. The *in vitro* cytotoxic activities of the complexes were tested against the human colorectal carcinoma cell line HCT 116.

2 | EXPERIMENTAL

2.1 | Materials and methods

Schiff base ligands (L1H to L6H) were prepared as previously reported.^[10–15] Palladium(II) chloride was purchased from Aldrich Chemicals. 3-(4,5-Dimethylthiazol-2-yl)-2,5-diphenyltetrazolium bromide (MTT) was purchased from Sigma-Aldrich, Germany. Commercial-grade solvents and reagents were used as supplied without further purification. Supercoiled pBR322 DNA and loading dye were purchased from Fermentas. CT DNA, agarose (molecular biology grade) and ethidium bromide (EB) were obtained from Sigma (St Louis, MO, USA). Elemental analysis was carried out using a PerkinElmer 2400 series-11 CHN/O analyser (Waltham, MA, USA). Quantitative determination of metal ions was carried out with a PerkinElmer model 3100 atomic absorption spectrometer. Infrared (IR), electronic (UV–visible), NMR and emission spectra were recorded with a PerkinElmer 2000 spectrometer; PerkinElmer Lambda 25 spectrometer; Bruker 500 MHz spectrometer at room temperature using deuterated dimethylsulfoxide (DMSO- d_6) as solvent and tetramethylsilane as internal standard; and a JASCO FP-750 spectrophotometer, respectively. Viscosity measurements were made using a Cannon Manning Semi-Micro viscometer (State College, PA, USA). Electrospray

ionization (ESI) mass spectra were obtained using an LC/MSD Trap VL (Agilent Technologies), which was operated in either positive ion or negative ion detection mode.

Synthesis of Ligands.

In brief, the Schiff base ligands were synthesized by refluxing a reaction mixture of hot ethanolic solutions (30 ml each) of 4-substituted 3-thiosemicarbazide (0.01 mol) and 5-substituted isatin (0.01 mol) for 2 h. The precipitates that formed during reflux were filtered and washed with cold ethanol.

Synthesis of Complexes.

The Pd(II) complexes were synthesized by refluxing a reaction mixture of hot ethanolic solutions (30 ml each) of PdCl₂ (0.01 mol) and appropriate ligand (0.01 mol) for 2 h. The precipitates that formed during reflux were filtered and washed with cold ethanol.

2.1.1 | C₁₅H₁₁ClPdN₄OS (PdL1)

Brown powder; m.p. > 300 °C; yield 88%. Anal. Calcd (%): C, 41.21; H, 2.54; N, 12.81; Pd, 24.34. Found (%): C, 41.53; H, 2.50; N, 12.85; Pd, 24.41. Selected IR data (KBr pellet, ν_{max} , cm⁻¹): 3306 to 2995 (NH), 1644 (C=O), 1550 (C=N), 769 (C–S). ¹H NMR (500 MHz, DMSO- d_6 , δ , ppm): 11.99 (s, 1 H, indole N-H), 11.28 (s, 1 H, CS-NH), 7.59 (s, 3 H, indole C2-H, thiosemicarbazide C11-H, C15-H), 7.48 to 7.43 (t, 3 H, indole C3-H, thiosemicarbazide C12-H, C14-H, $J = 6.5$ Hz), 7.24 to 7.15 (dt, 2 H, indole C4-H, thiosemicarbazide C13-H, $J = 7.0$ Hz), 7.03 (d, 1 H, indole C5-H, $J = 7.5$ Hz). ESI-MS (m/z): 435.9 (M⁻).

2.1.2 | C₁₆H₁₃ClPdN₄OS (PdL2)

Brown powder; m.p. > 300 °C; yield 80%. Anal. Calcd (%): C, 42.59; H, 2.90; N, 12.42; Pd, 23.58. Found (%): C, 42.71; H, 2.88; N, 12.73; Pd, 23.45. Selected IR data (KBr pellet, ν_{max} , cm⁻¹): 3332 to 3134 (NH), 1643 (C=O), 1586 (C=N), 753 (C–S). ¹H NMR (500 MHz, DMSO- d_6 , δ , ppm): 11.83 (s, 1 H, indole N-H), 11.22 (s, 1 H, CS-NH), 7.63 to 7.56 (dd, 2 H, C11-H, C15-H, $J = 7.6$ Hz), 7.46 to 7.44 (dd, 3 H, indole C5-H, thiosemicarbazide C12-H, C14-H, $J = 8.3$ Hz), 7.25 to 7.22 (t, 2 H, indole C3-H, thiosemicarbazide C13-H, $J = 7.5$ Hz), 6.90 (d, 1 H, indole C2-H, $J = 7.9$), 2.27 (s, 3 H, CH₃). ESI-MS (m/z): 449.0 (M – H)⁻.

2.1.3 | C₁₅H₁₀ClFPdN₄OS (PdL3)

Brown powder; m.p. > 300 °C; yield 79%. Anal. Calcd (%): C, 39.58; H, 2.21; N, 12.31; Pd, 23.38. Found (%): C, 39.70; H, 2.32; N, 12.39; Pd, 23.41. Selected IR data (KBr pellet, ν_{max} , cm⁻¹): 3415 to 3136 (NH), 1650 (C=O), 1552 (C=N), 768 (C–S). ¹H NMR (500 MHz, DMSO- d_6 , δ , ppm): 11.91

(s, 1 H, indole N-H), 11.30 (s, 1 H, CS-NH), 7.58 to 7.52 (dd, 3 H, indole C5-H, thiosemicarbazide C11-H, C15-H, $J = 8.0$), 7.47 to 7.44 (t, 2 H, thiosemicarbazide C12-H, C14-H, $J = 7.8$ Hz), 7.31 to 7.27 (dt, 2 H, indole C3-H, thiosemicarbazide C13-H, $J = 8.9$, 2.0 Hz), 7.02 to 7.00 (dd, 1 H, indole C2-H, $J = 8.6$, 4.2 Hz). ESI-MS (m/z): 455.0 ($M + 2H$)²⁺.

2.1.4 | C₁₀H₈ClPdN₅O₃S (PdL4)

Brown powder; m.p. > 300 °C; yield 84%. Anal. Calcd (%): C, 28.59; H, 1.92; N, 16.67; Pd, 25.33. Found (%): C, 28.33; H, 1.65; N, 16.43; Pd, 25.61. Selected IR data (KBr pellet, ν_{max} , cm⁻¹): 3290 (NH), 1641 (C=O), 1527 (C=N), 748 (C-S). ¹H NMR (500 MHz, DMSO-*d*₆, δ , ppm): 11.20 (s, 1 H, indole N-H), 9.59 to 9.56 (q, 1 H, CS-NH, $J = 9.7$, 4.8 Hz), 8.30 to 8.28 (dd, 1 H, indole C5-H, $J = 8.3$, 2.2 Hz), 8.26 to 8.24 (dd, 1 H, indole C3-H, $J = 8.5$, 2.4 Hz), 7.21 to 7.10 (t, 1 H, indole C2-H, $J = 8.5$ Hz), 3.10 (d, 3 H, thiosemicarbazide CH₃, $J = 4.9$ Hz). ESI-MS (m/z): 418.0 (M^-).

2.1.5 | C₁₁H₁₁ClPdN₄OS (PdL5)

Brown crystals; m.p. > 300 °C; yield 88%. Anal. Calcd (%): C, 33.95; H, 2.85; N, 14.40; Pd, 27.35. Found (%): C, 33.77; H, 2.59; N, 14.36; Pd, 27.52. Selected IR data (KBr pellet, ν_{max} , cm⁻¹): 3336 to 3245 (NH), 1635 (C=O), 1538 (C=N), 764 (C-S). ¹H NMR (500 MHz, DMSO-*d*₆, δ , ppm): 11.81 (s, 1 H, indole N-H), 9.35 to 9.32 (q, 1 H, CS-NH, $J = 9.2$, 4.6 Hz), 7.41 (d, 1 H, indole C5-H), 7.22 to 7.16 (dd, 1 H, indole C3-H, $J = 8$ Hz), 6.89 to 6.88 (d, 1 H, indole C2-H, $J = 8.0$ Hz), 3.07 (d, 3 H, thiosemicarbazide CH₃, $J = 5.0$ Hz), 2.30 (d, 3 H, indole CH₃, $J = 5.0$ Hz). ESI-MS (m/z): 388.0 ($M + H$)⁺.

2.1.6 | C₁₂H₁₃ClPdN₄OS (PdL6)

Brown powder; m.p. > 300 °C; yield 80%. Anal. Calcd (%): C, 35.75; H, 3.25; N, 13.90; Pd, 26.39. Found (%): C, 35.65; H, 3.55; N, 13.73; Pd, 26.60. Selected IR data (KBr pellet, ν_{max} , cm⁻¹): 3385 to 3342 (NH), 1636 (C=O), 1513 (C=N), 765 (C-S). ¹H NMR (500 MHz, DMSO-*d*₆, δ , ppm): 11.78 (s, 1H, indole N-H), 9.40 to 9.38 (t, 1H, CS-NH, $J = 5.3$ Hz), 7.39 (d, 1 H, indole C5-H, $J = 5.6$ Hz), 7.22 to 7.17 (dd, 1 H, indole C2-H, $J = 8.5$ Hz), 6.89 (d, 1 H, indole C3-H, $J = 7.9$ Hz), 3.53 to 3.49 (p, 2 H, thiosemicarbazide CH₂, $J = 6.5$ Hz), 2.29 (s, 3H, indole CH₃), 1.20 to 1.17 (t, 3H, thiosemicarbazide CH₃, $J = 7.6$ Hz). ESI-MS (m/z): 401.0 ($M - H$)⁻.

2.2 | X-ray crystallography

Single crystals of PdL5, suitable for diffraction, were grown by slow evaporation of 3:1 mixtures of acetone and DMSO. Selected crystal data and data collection parameters are presented in Table 1.

Data for the PdL5 complex were collected using a Bruker SMART APEX II CCD diffractometer^[16] equipped with graphite monochromatized Mo K α radiation ($\lambda = 0.71073$ Å) at 100(1) K. Multi-scan absorption corrections were applied using the SADABS program.^[16] The structure was solved by the direct method using the SHELXS-97 program.^[17] Refinements on F² were performed using SHELXL-97 by the full-matrix least-squares method with anisotropic thermal parameters for all non-hydrogen atoms. Nitrogen-bound hydrogen atoms were located in a difference Fourier map and refined freely. The remaining hydrogen atoms were positioned geometrically and refined using a riding model. The SHELXTL program^[17] was used for the pictorial representation of the structure.

TABLE 1 Crystallographic data for complex PdL5

Formula	C ₁₁ H ₁₁ ClN ₄ OPdS (C _{2.92} H ₆ OS _{0.08})
Formula weight	448.86
<i>T</i> (K)	100(1)
Crystal system	Triclinic
Space group	P-1
<i>a</i> (Å)	8.4311(1)
<i>b</i> (Å)	10.4885(1)
<i>c</i> (Å)	10.5347(1)
α (°)	109.588(1)
β (°)	103.743(1)
γ (°)	100.822(1)
<i>V</i> (nm ³)	815.334(18)
<i>Z</i>	2
<i>D_c</i> (mg m ⁻³)	1.828
<i>F</i> (000)	450
Crystal dimensions (mm)	0.09 × 0.12 × 0.31
θ range (°)	2.2–32.5
<i>hkl</i> ranges	–12 < <i>h</i> < 12 –15 < <i>k</i> < 15 –15 < <i>l</i> < 15
Data/parameters	5811/223
Goodness-of-fit on <i>F</i> ²	1.05
Final <i>R</i> indices [<i>I</i> > 2 σ (<i>I</i>)]	<i>R</i> ₁ = 0.0261 <i>wR</i> ₂ = 0.0609
Highest peak/deepest hole	$\Delta\rho_{\text{max}} = 0.79 \text{ e } \text{Å}^{-3} / \Delta\rho_{\text{min}} = -0.68 \text{ e } \text{Å}^{-3}$

2.3 | DNA interaction studies

DNA binding experiments, including absorption and emission spectral studies and viscosity measurements, conformed to the standard methods.^[18–21] Concentrated CT DNA stock solution was prepared in 5 mM Tris–HCl/50 mM NaCl in water at pH = 7.2. The DNA concentration per nucleotide was determined by absorption spectroscopy using the molar absorption coefficient ($6600 \text{ M}^{-1} \text{ cm}^{-1}$) at 260 nm.^[22] The purity of the CT DNA was verified using the ratio of the absorbance values at 260 and 280 nm in the respective buffer, which was found to be greater than 1.9. This result indicates that DNA was sufficiently free of protein. The stock solutions were stored at 4 °C and used within four days. The DNA binding experiments were performed at room temperature. All experiments were carried out by keeping the concentration of palladium complexes constant (50 μM), whereas the DNA concentration was varied (0 to 200 μM). An equal amount of DNA was added to the palladium complex cuvette and reference cuvette to eliminate the absorbance of CT DNA itself.^[23] Tris buffer was subtracted through baseline correction. UV–visible and emission spectra were recorded after equilibration for 10 min after each addition. Viscosity experiments were carried out using a thermostatically controlled water bath maintained at 37.0 ± 0.1 °C. The flow rates of Tris–HCl buffer (pH = 7.2), DNA (200 μM) and DNA in the presence of Pd(II) complexes at various concentrations (0 to 2.5×10^{-4} M) were measured three times each with a digital stopwatch, and the average flow time was calculated. Data are presented as $(\eta/\eta_0)^{1/3}$ versus the ratio of the concentration of complex to CT DNA, where η is the viscosity of DNA in the presence of complex and η_0 is that of DNA alone. Viscosity values were calculated from the observed flow time of DNA-containing solutions (t) corrected for that of buffer alone (5 mM Tris–HCl/50 mM NaCl) (t_0) using $\eta = (t - t_0)$.

2.4 | DNA cleavage studies

Cleavage experiments of supercoiled pBR322 DNA (0.5 μg) were performed at pH = 7.2 in 5 mM Tris–HCl/50 mM NaCl buffer. Oxidative DNA cleavage was monitored by treating pBR322 DNA with varying concentrations of Pd(II) complexes (0.1 to 1 mM) and H_2O_2 , followed by dilution with 5 mM Tris–HCl/50 mM NaCl buffer to a total volume of 20 μl . The experiment was carried out by adding scavenger (DMSO) for the hydroxyl radical species to a complex–DNA mixture to investigate the mechanism of DNA cleavage promoted by these complexes. The samples were incubated for 2 h at 37 °C. A loading dye was added, and electrophoresis was carried out at 50 V for 1 h in Tris–HCl buffer using 1% agarose gel. The resulting bands were stained with EB before being photographed under UV light.

2.5 | Anti-proliferative activity

2.5.1 | Preparation of cell culture

HCT 116 cells were allowed to grow under optimal incubator conditions. Cells that had reached a confluence of 70 to 80% were chosen for cell plating. Old medium was aspirated out of the plate, and cells were washed using sterile phosphate-buffered saline (pH = 7.4) two to three times. Phosphate-buffered saline was completely discarded after washing. Trypsin was added and evenly distributed onto the cell surface, and the cells were incubated at 37 °C in 5% CO_2 for 1 min. The flasks containing the cells were gently tapped to aid cell segregation, and observed under an inverted microscope (if cell segregation was unsatisfactory, the cells were incubated for another minute). Trypsin activity was inhibited by adding 5 ml of fresh complete medium (10% foetal bovine serum). Cells were counted and diluted to obtain a final concentration of 2.5×10^5 cells ml^{-1} , and seeded into wells (100 μl of cells per well). Finally, the cell-containing plates were incubated at 37 °C with an internal atmosphere of 5% CO_2 .

2.5.2 | MTT assay

Cancer cells (100 μl of cells per well, 1.5×10^5 cells ml^{-1}) were seeded on a 96-well microtiter plate, which was incubated with CO_2 overnight to allow cell attachment. The compounds were diluted with media into the required concentrations from the stock. Various concentrations (6.25 to 200 μM) of 100 μl of test substances were separately added to each well containing the cells. The plates were then incubated at 37 °C with an internal atmosphere of 5% CO_2 for 48 h. The plates were then treated with 20 μl of MTT reagent and incubated again for 4 h. Approximately 50 μl of MTT lysis solution (DMSO) was added to the wells, and the plates were further incubated for 5 min at room temperature. Finally, the absorbances at 570 and 620 nm were measured using a standard Infinite 200 PRO multimode microplate reader (Tecan, USA). Data were recorded and analysed to estimate the effects of test compounds on cell viability and growth inhibition. The percentage inhibition of cell proliferation was calculated from the optical density obtained from MTT assay. 5-Fluorouracil (5-FU) was used as a standard reference drug.^[24] Statistical differences between the treatments and control were evaluated by one-way ANOVA, followed by Tukey's multiple comparison test. Differences were considered significant at $p < 0.05$ and $p < 0.01$.

3 | RESULTS AND DISCUSSION

Complexes PdL1 to PdL6 were obtained in good yield from the reaction of Pd(II) with an appropriate Schiff base (L1H

to L6H; Scheme 1) in a 1:1 molar ratio in ethanol medium with reflux for 2 h (Scheme 2). These complexes were slightly soluble in common organic solvents, but soluble in dimethylformamide and DMSO.

Spectroscopic Analysis.

3.1 | IR spectra

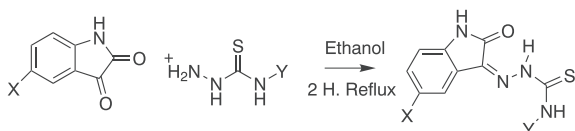
The characteristic IR bands recorded for the free ligands^[10] differed from those of the related complexes, and provided significant indications of the bonding sites of thiosemicarbazone ligands. Compared with the spectra of the Schiff bases, PdL1 to PdL6 exhibited the $\nu(\text{C}=\text{O})$ band from 1635 to 1650 cm^{-1} , showing a shift to lower wavenumbers. This finding indicates that the carbonyl oxygen was coordinated to the metal ion. The $\nu(\text{C}=\text{N})$ band from 1513 to 1586 cm^{-1} in the spectra of the metal complexes showed a shift to lower wavenumbers, which indicates that the nitrogen atom of the azomethine group was coordinated to the metal ion. This finding was further supported by the band at approximately 748 to 769 cm^{-1} for the metal complexes because of $\nu(\text{C}-\text{S})$.^[25] Thus, the IR spectral results for PdL1 to PdL6 provide strong evidence for the complexation of Schiff bases with metal ions in a tridentate mode as reported for similar structures.^[7]

3.2 | ^1H NMR spectra

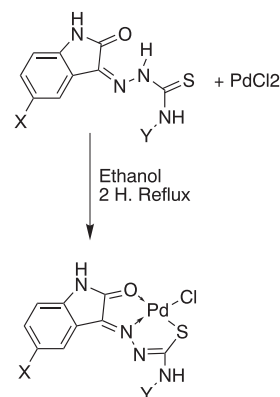
The ^1H NMR ($\text{DMSO}-d_6$) spectra of the Pd(II) complexes showed approximately the same peaks identical to those of the free ligands,^[10] except that the signal of thiosemicarbazide N—NH proton in the spectra of the ligands disappeared in the spectra of the complexes. This finding provides additional evidence of ligand deprotonation during metal chelation.

3.3 | Mass spectra

The mass spectra of PdL1, PdL2, PdL4 and PdL6 recorded in the negative mode showed the following peaks at ESI-MS (m/z): 435.9, 449.0, 418.0 and 401.0, respectively. These indicate the presence of $[\text{M}^-]$, $[\text{M} - \text{H}]^-$, $[\text{M}^-]$ and $[\text{M} - \text{H}]^-$, respectively. The mass spectra of PdL3 and PdL5 recorded in the positive mode showed peaks at ESI-



SCHEME 1 Synthetic route and structures for the Schiff base ligands L1H–L6H. L1: X = H, Y = Ph; L2: X = CH₃, Y = Ph; L3: X = F, Y = Ph; L4: X = NO₂, Y = CH₃; L5: X = CH₃, Y = CH₃; L6: X = CH₃, Y = CH₃CH₂



SCHEME 2 Synthetic route and structures for the compounds PdL1–PdL6. PdL1: X = H, Y = Ph; PdL2: X = CH₃, Y = Ph; PdL3: X = F, Y = Ph; PdL4: X = NO₂, Y = CH₃; PdL5: X = CH₃, Y = CH₃; PdL6: X = CH₃, Y = CH₃CH₂

MS (m/z) of 455.0 and 388.0, respectively, indicating the presence of these complexes as $[\text{M} + 2\text{H}]^+$ and $[\text{M} + \text{H}]^+$.

3.4 | Crystal structure of PdL5

The molecular structure of compound PdL5 and the atom numbering scheme are shown in Figure 1. The PdL5 complex presented a square planar geometry, which was slightly distorted around the palladium atom. The basal plane was occupied by the S(1), O(1) and N(2) atoms of the ligand and Cl(1) ion. Distortion from square planar geometry was evident from the bond angles S(1)–Pd(1)–N(2) = 83.92(5)°,

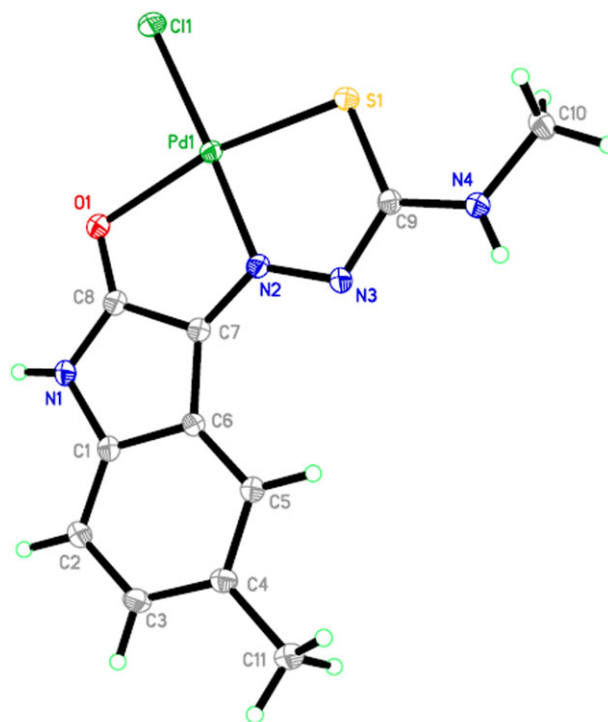


FIGURE 1 Structure of complex PdL5, showing 50% probability displacement ellipsoids and atomic numbering

Cl(1)–Pd(1)–S(1) = 98.24(2)°, Cl(1)–Pd(1)–O(1) = 94.14(4)°, O(1)–Pd(1)–N(2) = 83.72(6)°, S(1)–Pd(1)–O(1) = 167.60(4)° and Cl(1)–Pd(1)–N(2) = 177.40(5)°; and bond lengths Pd(1)–S(1) = 2.2314(5) Å, Pd(1)–N(2) = 1.9726(15) Å, Pd(1)–O(1) = 2.1339(14) Å and Pd(1)–Cl(1) = 2.3030(5) Å. The unit cell contained a non-integer number of atoms (C_{2.92}H₆OS_{0.08}) because of partially occupied (solvent) sites and substitutional disorder. In crystal packing (Figure 2), the molecules were interconnected through intermolecular hydrogen bonds. A weak bond between S(2) and Pd(1) with Pd–S = 3.794 Å was also observed, which changed the coordination geometry around Pd(1) from square planar to pseudo square pyramidal.

3.5 | DNA interaction studies

3.5.1 | Absorption spectral studies

One of the most useful techniques for studying the DNA binding of molecules is electronic absorption spectroscopy. DNA usually results in hypochromism and red shifting (bathchromism) as a consequence of the intercalation mode involving a strong stacking interaction between an aromatic chromophore and the DNA base pairs.^[26] This phenomenon arises from the contraction of CT DNA in the helix axis and conformational changes.^[27,28] Hyperchromism results from the secondary distortion of the DNA double-helix structure.^[29,30] The extent of hyperchromism indicates partial or non-intercalative binding modes.^[31] The absorption spectra of 50 μM PdL3 and PdL5 in the absence and presence of CT DNA (0 to 200 μM) are shown in Figures 3 and 4. The absorption spectra of PdL1, PdL2, PdL4 and PdL6 are given in the supporting information (Figures S1–S4). The absorption spectra of PdL2, PdL5 and PdL6 displayed clear hypochromism with a slight red shift of approximately 1 to 3 nm. After the compounds intercalated to the DNA base pairs, the π* orbitals of the intercalated compounds coupled

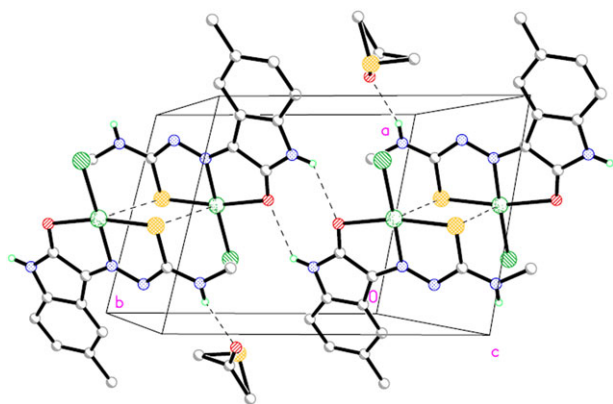


FIGURE 2 Crystal packing of PdL5, viewed approximately along the *c*-axis

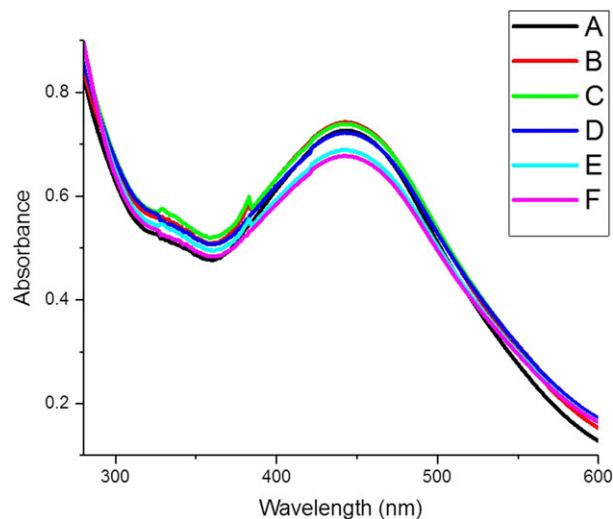


FIGURE 3 Absorption spectra of PdL3 in the absence and in the presence of increasing amounts of DNA in Tris–HCl buffer (pH = 7.2). [PdL3] = 50 μM; [DNA]: A, 2.861×10^{-5} ; B, 5.666×10^{-5} ; C, 8.417×10^{-5} ; D, 1.1115×10^{-4} ; E, 1.3761×10^{-4} ; F, 1.6358×10^{-4} M

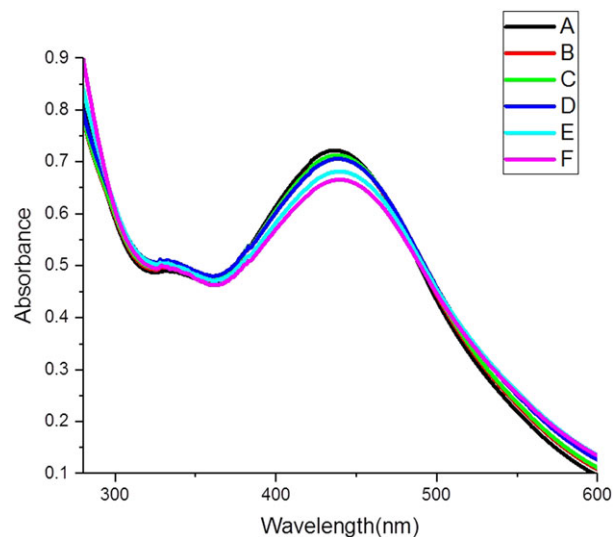


FIGURE 4 Absorption spectra of PdL5 in the absence and in the presence of increasing amounts of DNA in Tris–HCl buffer (pH = 7.2). [PdL5] = 50 μM; [DNA]: A, 2.861×10^{-5} ; B, 5.666×10^{-5} ; C, 8.417×10^{-5} ; D, 1.1115×10^{-4} ; E, 1.3761×10^{-4} ; F, 1.6358×10^{-4} M

with the π orbitals of the base pairs, thereby decreasing the π → π* transition energies. These interactions result in the observed hypochromism.^[32] The hypochromism of these complexes followed the order of PdL2 = PdL5 > PdL6. By contrast, PdL1, PdL3 and PdL4 exhibited both hypochromism and hyperchromism at approximately 382 to 442 nm and 243 to 358 nm, respectively; this phenomenon suggests the distortion of the DNA double-helix structure after the complex binds to DNA through the intercalation

mode.^[33] This behaviour has been reported for chiral Schiff base complexes^[34,35] and PdCl₂(LL).^[36] Complexes PdL1 and PdL6 showed hypochromism with a small red shift of approximately 1 nm, whereas PdL2, PdL3 and PdL5 displayed red shifts of approximately 3 nm, and PdL4 showed a high red shift of approximately 5 nm.

The intrinsic binding constant of all complexes with DNA was determined by observing the changes in absorbance of the complexes with increased DNA concentration using the following equation^[30,37]:

$$\frac{[\text{DNA}]}{\varepsilon_a - \varepsilon_f} = \frac{[\text{DNA}]}{\varepsilon_b - \varepsilon_f} + \frac{1}{K_b(\varepsilon_b - \varepsilon_f)}$$

<NI>where ε_a , ε_f and ε_b are the extinction coefficients observed for the absorption band at a given DNA concentration for free and bound complexes, respectively; [DNA] is the DNA concentration in base pairs; and K_b is the intrinsic binding constant determined from the slope-to-intercept ratio of a plot of $[\text{DNA}]/(\varepsilon_a - \varepsilon_f)$ versus [DNA] (Figures S3 and S4). The K_b values for PdL1, PdL2, PdL3, PdL4, PdL5 and PdL6 were 1.79×10^6 , 2.69×10^5 , 1.55×10^6 , 5.78×10^4 , 3.14×10^5 and $4.93 \times 10^5 \text{ M}^{-1}$, respectively. The K_b values of the complexes PdL1, PdL2, PdL3, PdL5 and PdL6 were close to those reported for typical classical intercalators,^[38] whereas that of complex PdL4 was much smaller. This behaviour reflects that the DNA binding affinities of PdL1, PdL2, PdL3, PdL5 and PdL6 were stronger than that of PdL4. The DNA binding abilities of PdL1 and PdL3 were higher than those of the other complexes. This result was attributed to the effective stacking interaction in the former because of the presence of an extended aromatic phenyl ring, which allowed an intercalating ligand deep in the DNA base pairs. A comparison of the intrinsic binding constants of these complexes with those of DNA-intercalative Pd(II) complexes, such as $[\text{Pd}(\text{dmphen})(\text{CO}_3)]\text{H}_2\text{O}$ ^[39] and $[\text{Pd}(\text{bpy})(\text{pip-dtc})]\text{NO}_3$,^[40] revealed that these complexes bind to DNA by intercalation, but the binding mode requires more experiments.

3.5.2 | Emission spectral studies

Fluorescence titration experiments were performed to further study the interaction mode between PdL1–PdL6 and CT DNA. These complexes could emit luminescence in Tris–HCl/NaCl buffer at room temperature with maximum wavelength of approximately 379 nm (supporting information, Figs S5–S8). The emission spectra of PdL2 and PdL4 (50 μM) in the absence and presence of CT DNA (0 to 200 μM) are shown in Figures 5 and 6. The emission intensity increased with increasing CT DNA concentration. These observations imply that these complexes could strongly

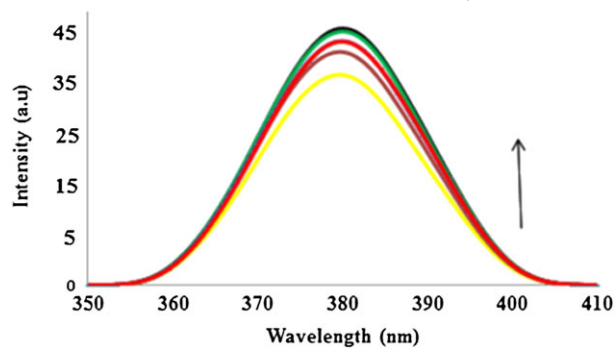


FIGURE 5 Emission spectra of PdL2 in the absence and in the presence of increasing amounts of DNA in Tris–HCl buffer (pH = 7.2). [PdL2] = 50 μM ; [DNA] = 0–163.58 $\times 10^{-6}$ M. The arrow shows the emission intensity increasing upon increasing the CT DNA concentration

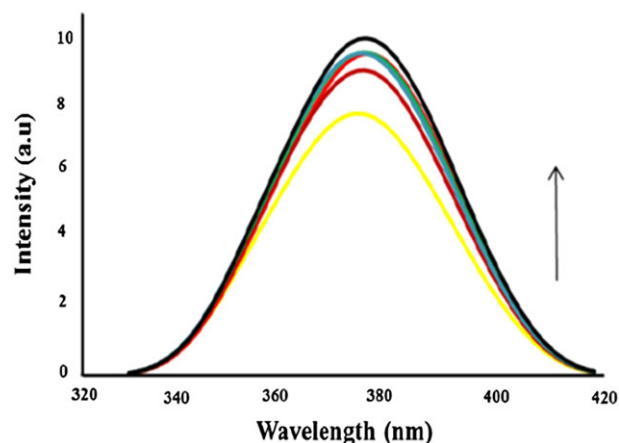


FIGURE 6 Emission spectra of PdL4 in the absence and in the presence of increasing amounts of DNA in Tris–HCl buffer (pH = 7.2). [PdL4] = 50 μM ; [DNA] = 0–163.58 $\times 10^{-6}$ M. The arrow shows the emission intensity increasing upon increasing the CT DNA concentration

interact with CT DNA, and indicate an intercalative mode with the base pairs of the DNA helix.^[41]

3.5.3 | Viscosity measurements

The most critical and least ambiguous tests of binding in solution in the absence of crystallographic data^[42,43] are hydrodynamic measurements (i.e. viscosity and sedimentation), which are sensitive to length changes. A classical intercalation molecule, such as EB, lengthens the DNA helix, leading to increased DNA viscosity caused by an increase in the separation of base pairs at the interaction site and an increase in the overall double-helix length. Partial or non-classical intercalation of a complex results in the bending of the DNA helix that decreases the effective DNA length and

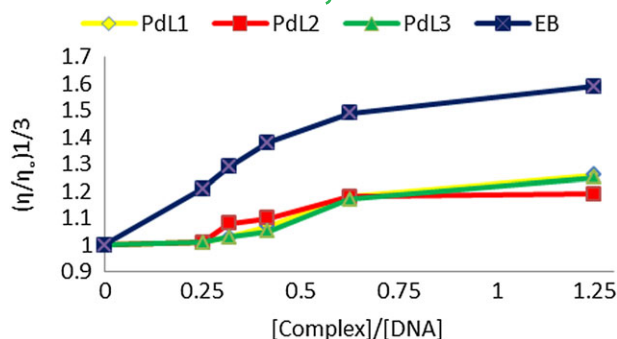


FIGURE 7 Effect of increasing amounts of EB, PdL1, PdL2 and PdL3 on the relative viscosity of CT DNA at 37.0 ± 0.1 °C

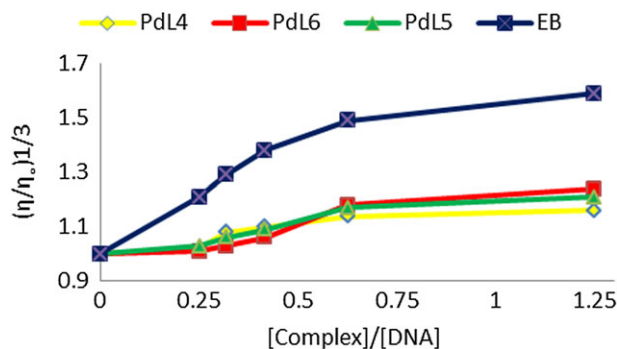


FIGURE 8 Effect of increasing amounts of EB, PdL4, PdL5 and PdL6 on the relative viscosity of CT DNA at 37.0 ± 0.1 °C

viscosity. By contrast, an electrostatic or groove binding mode has minimal effects on DNA viscosity.^[44,45] The viscosity measurements of PdL1–PdL6 and EB are shown in Figures 7 and 8. A plot of relative specific viscosity versus the [complex]/[DNA] ratio showed a significant increase upon addition of the complexes. These observations suggest the intercalative binding of these complexes to the DNA

double helix,^[46,47] which agree with the results of the optical absorption experiments.

3.5.4 | DNA cleavage studies

The degree to which complexes PdL1–PdL6 could function as DNA cleavage agents was examined using supercoiled pBR322 DNA ($0.5 \mu\text{g } \mu\text{l}^{-1}$) as the target. The cleavage efficiency of these complexes was investigated through agarose gel electrophoresis using different concentrations of complexes (supporting information, Figs S9–S12) in 1% DMSO/5 mM Tris–HCl/50 mM NaCl buffer at pH = 7.2, with and without H_2O_2 , and incubation of 2 h. The activity of the complexes was estimated by the conversion of DNA from Form I to Forms II and III. The fastest migration is detected in the supercoiled form (Form I). If only one strand is cleaved, the supercoils relax to convert into a slower-moving nicked form (Form II). If both strands are cleaved, a linear form (Form III) is produced, which migrates between Forms I and II.^[48]

3.5.5 | Oxidative cleavage

This experiment was conducted in the presence of H_2O_2 as an oxidizing agent. The control experiment did not show any apparent cleavage of DNA (lane 2). In the presence of the complexes at different concentrations (lanes 4 to 12), the plasmid DNA was converted from Form I to Forms II and III at 0.1 mM (lane 4 for PdL1 (Figure 9), and PdL3), 0.3 mM (lane 6 for PdL2) and 0.6 mM (lane 8 for PdL4). The plasmid DNA was converted from Form I to Form II at 0.1 mM (lane 4 for PdL5 and PdL6). DNA was completely degraded above these concentrations. The reactions were allowed to proceed in the presence of DMSO as hydroxyl radical scavenger (lane 3) to investigate the DNA cleavage mechanism promoted by these complexes.^[49] The addition of the hydroxyl radical scavenger completely inhibits the

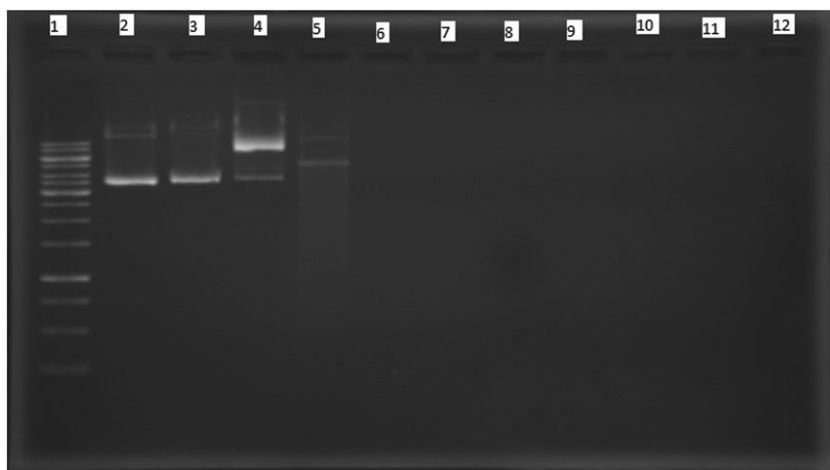


FIGURE 9 Cleavage of supercoiled pBR322 ($0.5 \mu\text{g } \mu\text{l}^{-1}$) at different concentrations of PdL1 in Tris–HCl buffer (pH = 7.2) for 2 h at 37 °C. Lane 1: DNA ladder; lane 2: DNA + H_2O_2 ; lane 3: DNA + PdL1 (1 mM) + DMSO; lanes 4–12: DNA with increasing the concentrations of PdL1 + H_2O_2 (0.1–1 mM) + buffer

DNA cleavage activity (PdL4, Figure 10), which is induced by these complexes. This observation suggests the involvement of the hydroxyl radical in cleavage.^[50]

3.5.6 | Anti-proliferative activity

The *in vitro* anti-proliferative activity of PdL1–PdL6 was evaluated against HCT 116 cells. The effects of various concentrations of the complexes on HCT 116 cells after 48 h of treatment are shown in Figure 11. The anticancer efficiencies of all tested compounds are summarized in Table 2. Results of the anti-proliferation test show that all tested compounds had a dose-dependent effect. Figure 12 shows photomicrographic images of cancer cells treated with these compounds for 48 h. First, cells treated with the standard drug 5-FU ($IC_{50} = 7.3 \mu\text{M}$) showed decreased viability. The HCT 116 cells treated with PdL1 exhibited the most potent anti-proliferative activity ($IC_{50} = 11 \mu\text{M}$) among all the synthesized compounds tested. Cell growth was clearly affected by the treatment. The results could be compared with the standard reference $^{[51]}$ -FU. Except for a few affected cells, the activity was so pronounced that only cellular debris remained in the growth medium. HCT 116 cells treated with PdL2 showed considerable cytotoxicity with $IC_{50} = 51.4 \mu\text{M}$. The reduction in the population doubling time could be clearly visualized from the reduced number of viable cells. Treatment with PdL3 showed a significant inhibitory effect on the proliferation of HCT 116 cells ($IC_{50} = 16 \mu\text{M}$). The effect could be compared with the standard reference $^{[51]}$ -FU. The treatment caused an abnormality in cellular morphology of treated cells, and rendered cells with round shapes. The photomicrographic images of HCT 116 cells show the effect of PdL4. The compound displayed moderate cytotoxicity as the IC_{50} value (112 μM) was higher than that of the other samples tested. HCT 116 cells treated with PdL5 showed a significant cytotoxic effect ($IC_{50} = 46 \mu\text{M}$). The treatment

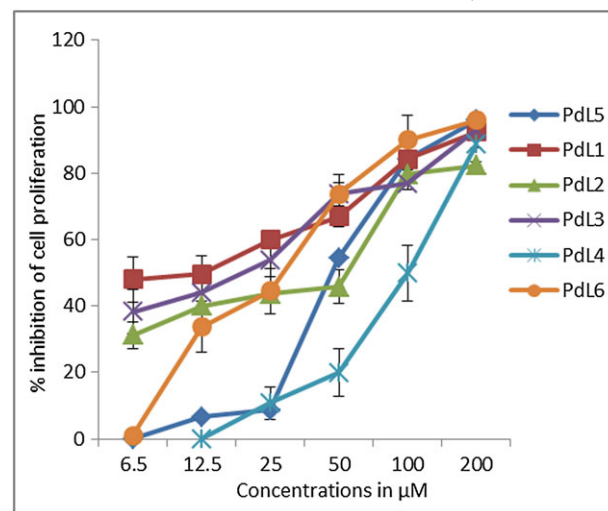


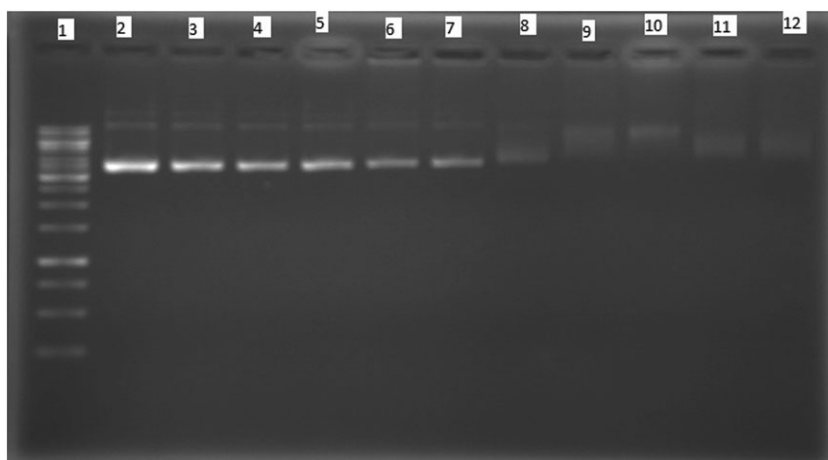
FIGURE 11 Effect of different concentrations of PdL1–PdL6 on human colorectal cancer cells (HCT 116) after 72 h treatment

TABLE 2 Anticancer efficiencies of tested compounds

Compound	IC_{50} value (μM)
PdL1	11.0
PdL2	51.4
PdL3	16.0
PdL4	112.0
PdL5	46.0
PdL6	28.0

significantly ($p < 0.05$) affected cellular morphology and growth compared with the control. Finally, the treatment with PdL6 showed a significant ($p < 0.05$) cytotoxic effect on the proliferation of HCT 116 cells. The cells showed an abnormal cellular membrane with affected pseudopodial projections. Thus, cell growth was severely affected and presented a significantly low IC_{50} value (28 μM).

FIGURE 10 Cleavage of supercoiled pBR322 ($0.5 \mu\text{g} \mu\text{l}^{-1}$) at different concentrations of PdL4 in Tris–HCl buffer ($\text{pH} = 7.2$) for 2 h at 37 °C. Lane 1: DNA ladder; lane 2: DNA + H_2O_2 ; lane 3: DNA + PdL4 (1 mM) + DMSO; lanes 4–12: DNA with increasing the concentrations of PdL4 + H_2O_2 (0.1–1 mM) + buffer



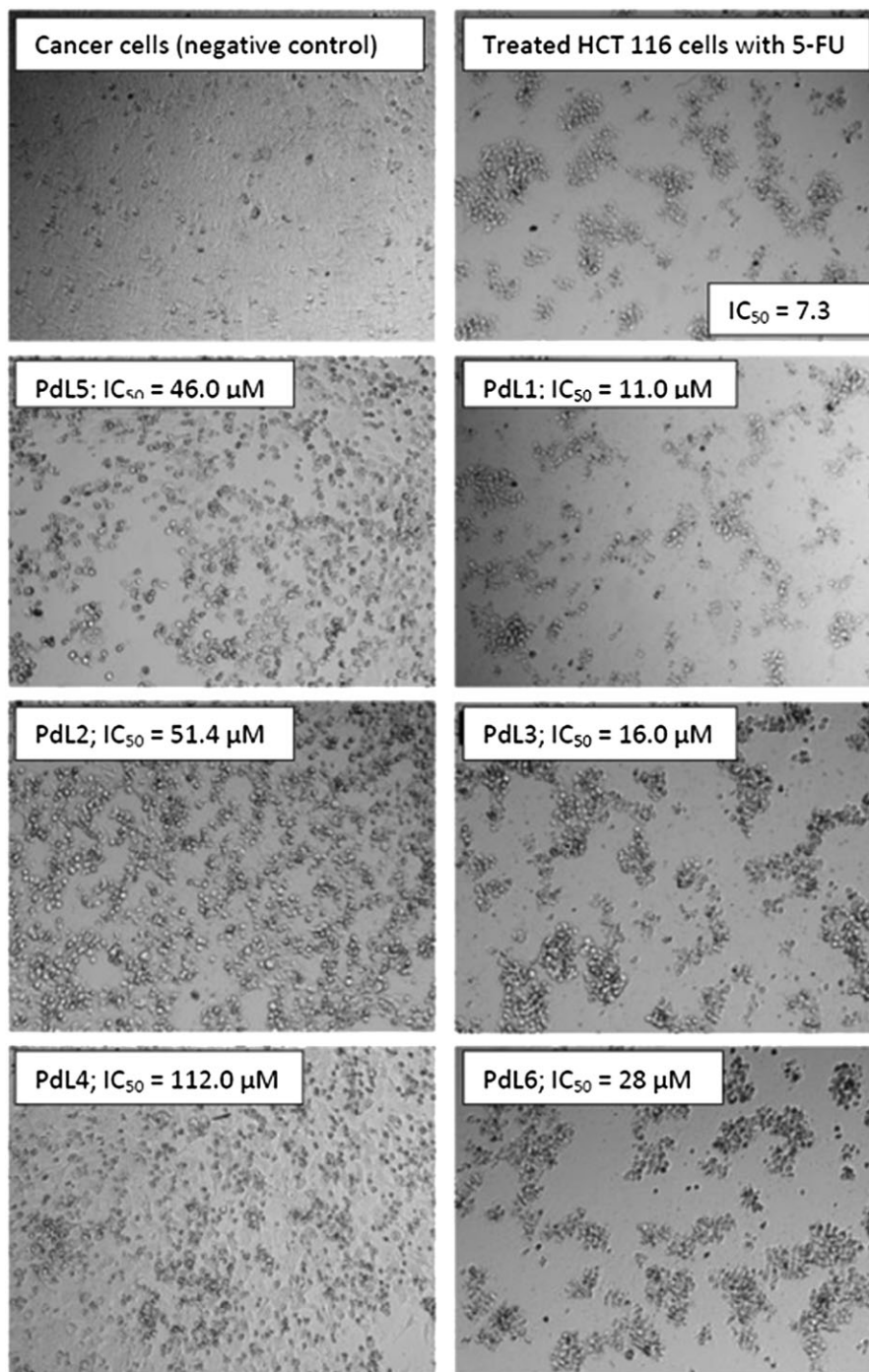


FIGURE 12 Images of cancer cells treated with complexes PdL1–PdL6 for 48 h

4 | CONCLUSIONS

Six novel square planar palladium(II) complexes (i.e. PdL1–PdL6) with tridentate ligands were synthesized and characterized using elemental analysis and various spectroscopic techniques. The crystal structure of PdL5 showed that it was a four-coordinate complex with a slightly distorted square planar geometry. The results of binding studies show that these complexes interacted with CT DNA through an intercalative

mode, which was investigated using absorption (K_b ranged from 5.78×10^4 to $1.79 \times 10^6 \text{ M}^{-1}$) and fluorescence spectra and viscosity measurements. Their affinity to DNA followed the order of PdL1 > PdL3 > PdL6 > PdL5 > PdL2 > PdL4, which could be attributed in some instances to the presence of an extended aromatic phenyl ring that allows an intercalating ligand deep in the DNA base pairs.^[50] The results of gel electrophoresis experiments indicate that these complexes could induce cleavage of plasmid DNA. Cleavage of DNA

by these complexes was dependent on concentration. All complexes showed nuclease activity in the presence of an oxidant, which may be due to free radical reaction (OH^\bullet) with DNA. Finally, the results of *in vitro* anti-proliferative activity against HCT 116 cells show dose-dependent cytotoxicity of the synthesized complexes, with significantly low IC_{50} ranging from 11.0 to 112.0 μM . Thus, the palladium(II) complexes of thiosemicarbazone Schiff bases with isatin moiety are promising anti-neoplastic agents.

ACKNOWLEDGEMENTS

The authors thank the Malaysian Government and Universiti Sains Malaysia for the RU research grant (1001/PKIMIA/815067). A.Q.A. thanks the Ministry of Higher Education and the University of Sebha (Libya) for a scholarship.

REFERENCES

- [1] A. S. Abu-Surrah, M. Kettunen, *Curr. Med. Chem.* **2006**, *13*, 1337.
- [2] S. Rafique, M. Idrees, A. R. Nasim, H. Akbar, A. Athar, *Biotechnol. Mol. Biol. Rev.* **2010**, *5*, 38.
- [3] E. Ramachandran, P. Kalaivani, R. Prabhakaran, M. Zeller, J. H. Bartlett, P. O. Adero, T. R. Wagner, K. Natarajan, *Inorg. Chim. Acta* **2012**, *385*, 94.
- [4] A. A. Shoukry, M. S. Mohamed, *Spectrochim. Acta A* **2012**, *96*, 586.
- [5] N. Sharama, D. P. Pathak, *Int J Pharm Pharm Sci* **2016**, *8*, 27.
- [6] M. Kasprzak, M. Fabijańska, L. Ch cińska, L. Szmigiero, J. Ochocki, *Molecules* **2016**, *21*, 455.
- [7] W. Hernández, A. J. Vaisberg, M. Tobar, M. Álvarez, J. Manzur, Y. Echevarría, E. Spodine, *New J. Chem.* **2016**, *40*, 1853.
- [8] P. Pakravan, S. Masoudian, *Iran. J. Pharm. Res.* **2015**, *14*, 111.
- [9] A. N. Patange, U. M. Yadav, P. A. Desai, P. U. Singare, *Int. Lett. Chem. Phys. Astron.* **2015**, *52*, 22.
- [10] A. Q. Ali, S. G. Teoh, A. Salhin, N. E. Eltayeb, M. K. Ahamed, A. M. S. Abdul Majid, *Spectrochim. Acta A* **2014**, *125*, 440.
- [11] A. Q. Ali, N. E. Eltayeb, S. G. Teoh, A. Salhin, H. K. Fun, *Acta Crystallogr.* **2012**, *E68*, o962.
- [12] A. Q. Ali, N. E. Eltayeb, S. G. Teoh, A. Salhin, H.-K. Fun, *Acta Crystallogr.* **2011**, *E67*, o3476.
- [13] A. Q. Ali, N. E. Eltayeb, S. G. Teoh, A. Salhin, H.-K. Fun, *Acta Crystallogr.* **2012**, *E68*, o285.
- [14] A. Q. Ali, N. E. Eltayeb, S. G. Teoh, A. Salhin, H.-K. Fun, *Acta Crystallogr.* **2012**, *E68*, o953.
- [15] A. Q. Ali, N. E. Eltayeb, S. G. Teoh, A. Salhin, H.-K. Fun, *Acta Crystallogr.* **2012**, *E68*, o955.
- [16] Bruker, APEX2, SAINT and SADABS, Bruker AXS Inc, Madison, WI **2005**.
- [17] G. M. Sheldrick, *Acta Crystallogr.* **2008**, *A64*, 112.
- [18] E.-J. Gao, L. Wang, M.-C. Zhu, L. Liu, W.-Z. Zhang, *Eur. J. Med. Chem.* **2010**, *45*, 311.
- [19] W. C. Chen, L. D. Wang, Y. T. Li, Z. Y. Wu, C. W. Yan, *Transition Met. Chem.* **2012**, *37*, 569.
- [20] A. Hussain, S. Gadadhar, T. K. Goswami, A. A. Karande, A. R. Chakravarty, *Eur. J. Med. Chem.* **2012**, *50*, 319.
- [21] M. N. Dehkordi, A. K. Bordbar, P. Lincoln, V. Mirkhani, *Spectrochim. Acta A* **2012**, *90*, 50.
- [22] H. Paul, T. Mukherjee, M. G. B. Drew, P. Chattopadhyaya, *J. Coord. Chem.* **2012**, *65*, 1289.
- [23] Y. Li, Z. Y. Yang, M. F. Wang, *J. Fluoresc.* **2010**, *20*, 891.
- [24] T. Mosmann, *J. Immunol. Methods* **1983**, *65*, 55.
- [25] D. A. I. Wiles, B. A. Gingras, T. Suprnchuk, *Can. J. Chem.* **1907**, *45*, 469.
- [26] L. M. Chen, J. Liu, J. C. Chen, C. P. Tan, S. Shi, K. C. Zheng, L. Nian, *Inorg. Biochem.* **2008**, *102*, 330.
- [27] G. Dehghan, M. Arvin, M. Ali, H. Pourfeizi, *International Conference on Medical, Biological and Pharmaceutical Sciences (ICMBPS '2011)*, Pattaya, Thailand **2011** 499.
- [28] R. Eshkourfu, B. Čobeljić, M. Vujčić, I. Turel, A. Pevec, K. Sepčić, M. Zec, R. T. S. Radić, D. Mitić, K. Andjelković, D. Sladić, *J. Inorg. Biochem.* **2011**, *105*, 1196.
- [29] N. Lingthoingambi, N. Rajen Singh, M. Damayanti, *J. Chem. Pharm. Res.* **2011**, *3*, 187.
- [30] L. Leelavathy, S. Anbu, M. Kandaswamy, N. Karthikeyan, N. Mohan, *Polyhedron* **2009**, *28*, 903.
- [31] J. Lu, Q. Sun, J.-L. Li, W. Gu, J.-L. Tian, X. Liu, S.-P. Yan, *J. Coord. Chem.* **2013**, *66*, 3280.
- [32] D. S. Raja, N. S. P. Bhuvanesh, K. Natarajan, *Inorg. Chim. Acta* **2012**, *385*, 81.
- [33] N. Shahabadi, S. Kashanian, A. Fatahi, *Bioinorg. Chem. Appl.* **2011**, *2011*, 687571.
- [34] N. H. Khan, N. Pandya, M. Kumar, P. K. Bera, R. I. Kureshy, S. H. R. Abdi, H. C. Bajaj, *Org. Biomol. Chem.* **2010**, *8*, 4297.
- [35] N. H. Khan, N. Pandya, N. C. Maity, M. Kumar, R. M. Patel, R. I. Kureshy, S. H. R. Abdi, S. Mishra, S. Das, H. C. Bajaj, *Eur. J. Med. Chem.* **2011**, *46*, 5074.
- [36] S. Kashanian, N. Shahabadi, H. Roshanfekar, K. Shalmashi, K. Omidfar, *Biochemistry* **2008**, *73*, 929.
- [37] S. Rajalakshmi, T. Weyhermüller, A. J. Freddy, H. R. Vasanthi, B. U. Nair, *Eur. J. Med. Chem.* **2011**, *46*, 608.
- [38] C. Icse, V. T. Yilmaz, *J. Photochem. Photobiol. B* **2014**, *130*, 115.
- [39] H. Mansouri-Torshizi, M. Eslami-Moghadam, A. Divsalar, A. Saboury, *Acta Chim. Slov.* **2011**, *58*, 811.
- [40] R. Palchaudhuri, P. J. Hergenrother, *Chem. Biotechnol.* **2007**, *18*, 497.
- [41] M. Tarui, M. Doi, T. Ishida, M. Inoue, S. Nakaike, K. Kitamura, *Biochemistry* **1994**, *304*, 271.
- [42] H. Guo, J. Lu, Z. Ruan, Y. Zhang, Y. Liu, L. Zang, J. Jiang, J. Huang, *J. Coord. Chem.* **2012**, *65*, 191.
- [43] L. B. Liaoa, H. Y. Zhou, X. M. Xiao, *J. Mol. Struct.* **2005**, *749*, 108.

- [44] N. Raman, S. Sobha, *J. Serb. Chem. Soc.* **2010**, *75*, 773.
- [45] S. Kashanian, M. Mehdi, K. P. Pakravan, H. Adibi, *Mol. Biol. Rep.* **2012**, *39*, 3853.
- [46] F. Liu, K. Wang, G. Bai, Y. Zhang, L. Gao, *J. Inorg. Chem.* **2004**, *43*, 1799.
- [47] L. Jin, P. Yang, *Microchem. J.* **1998**, *58*, 144.
- [48] P. Jogi, M. Padmaja, K. V. T. S. Pavan Kumar, C. Gyanakumari, *Chem. Pharm. Res.* **2012**, *4*, 1389.
- [49] F. Arjmand, S. Parveen, M. Afzal, L. Toupet, T. B. Hadda, *Eur. J. Med. Chem.* **2012**, *49*, 141.
- [50] E. Sundaravadivel, M. Kandaswamy, B. Varghese, *Polyhedron* **2013**, *61*, 33.

SUPPORTING INFORMATION

Additional Supporting Information may be found online in the supporting information tab for this article.

How to cite this article: Ali AQ, Teoh SG, Eltayeb NE, Khadeer Ahamed MB, Abdul Majid AMS, Almutaleb AAA. Synthesis, structure and *in vitro* anticancer, DNA binding and cleavage activity of palladium (II) complexes based on isatin thiosemicarbazone derivatives. *Appl Organometal Chem.* 2017;e3813. <https://doi.org/10.1002/aoc.3813>